

COMPRESSION PRE-STRESS OF TUBULAR TORSION SPRINGS

Vinko Močilnik, Nenad Gubelj, Jožef Predan, Jože Flašker

Original scientific paper

This paper reports the results of a series of biaxial static compression and torsion experiments performed to evaluate the effects of static compression stress on the fatigue life of those smooth tubes made of high strength spring steel. The fatigue life of biaxial loaded springs depends, among others, on biaxial compression and torsion loading. A high shear loading ratio leads to low-cycle fatigue behaviour rather than high-cycle fatigue, because it was found that a crack was initiated at a local highly deformed area on surface of the specimen. The experimentally obtained results show a significant extension of fatigue strain life as a result of combining axial compression loading with torsion. Cracking behaviour was observed and it was noted that compression pre-stresses contribute to retardation of the fatigue crack initiation process and, consequently, contribute to the extension of fatigue life.

Keywords: *fatigue, fatigue life, micro crack, multi axial stress state, pre-stressing, torsion, torsion bar spring, twist angle*

Tlačno prednaprežanje cjevastih torzijskih opruga

Izvorni znanstveni članak

U ovom se radu iznose rezultati niza eksperimenata dvoosnog statičkog tlačnog i torzijskog opterećenja kako bi se procijenilo djelovanje omjera tlačne napetosti na zamorni vijek trajanja cijevi napravljenih od visoko čvrstog čelika za opruge. Vijek trajanja dvoosno opterećenih opruga obzirom na zamor ovisi, između ostaloga, o biaksijalnom tlačnom i torzijskom opterećenju. Omjer opterećenja kod visokog smičnog naprežanja dovodi do nisko cikličkog više nego visoko cikličkog zamora jer se ustanovilo da se pukotina pojavila na lokalnom krajnje deformiranom dijelu na površini uzorka. Eksperimentalno dobiveni rezultati pokazuju značajan produžetak vijeka trajanja deformacije zbog zamora kao rezultat kombiniranja aksijalnog tlačnog i torzijskog opterećenja. Primijećena je pojava pukotina i zapaženo da tlačna prednaprežanja dovode do usporavanja procesa nastajanja zamornih pukotina i stoga doprinose produženju vijeka trajanja obzirom na zamor.

Ključne riječi: *kut uvijanja, mikropukotina, prednaprežanje, torzija, torzijska opruga, vijek trajanja obzirom na zamor, višeosno stanje naprežanja, zamor*

1

Introduction

Uvod

The spring's fatigue life is affected by many factors such as the spring's steel quality, the spring's manufacturing process, surface quality and the maximum torsion stress. It is accepted that the enlargement of a torsion spring's life is achieved by cold rolling of its surface and pre-stressing, where a higher elastic limit and higher working angle of the spring [1] is extremely important. The fatigue life enlargement of the tubular springs can be achieved by pre-stressing with constant compression force in axial direction, Fig. 1. The advantage of the tubular torsion springs is in the fact that the destruction does not appear unexpectedly and they can be loaded alternately. In such a way the tubular spring's body is loaded by multi-axial stress state.

There are several papers treating problems of combined loading with torsion and axle force on tubular specimens. Longer continued growth of a crack and its closure in a tip was stated under loading mode III; Tschegg [2]. Fonte and Freitas [3] analysed the response of stainless steel and the spring's steel to fatigue at the combination of loading modes I and III [4]. Makabe and Socie [5] were testing steel 4340 under the conditions of simulating loading III and I. It was stated that the crack branching was subject to micro cracks forming and to loading size and that the crack branches do not continue symmetrically regarding the initial crack. The authors Yang and Kuang [6] were studying the cracks' shapes and their growth rate on steel specimens of quality S45 under various combinations of torsion and constant axial force loading effects. They stated that the crack propagation angle is of about 45° for various loading amplitudes, that the static tension axial force causes together with cyclic torsion an accelerated growth of a crack

and it lowers the fatigue life, that the compression axial force together with torsion considerably enlarges the fatigue life and it does not affect the crack's propagation angle. It was stated as well that the crack's propagation direction depends on alternating stress and it does not depend on medium stress, while the fatigue life depends on it.

The authors Tanaka, Iwata and Akiniwa [7] were testing the tubular specimens made of lead-free solder under torsion and a combination of torsion-compression loading in axial direction. It was stated that in the first case the crack propagates in the direction of the maximum shear stress, and in the second case in the direction rectangular on the principal stresses. Lots of micro cracks are formed during individual phases inside the material lattice, and later on they are united in the main crack.

The authors Bjerken and Melin [8] have developed a method to investigate the growth of micro structurally short crack in a ductile crystalline material. The crack itself is modelled by a distribution of dislocation dipoles of finite length, while the local plasticity is developed by the emission and annihilation of discrete dislocations. Investigations of a short edge crack growing have shown that the competition between increasing global stress due to crack advance and the increasing shielding effect in the crack tip from the dislocations in the plastic zone is crucial for crack growth. The distance between the crack tip and a grain boundary is shown to influence the crack growth characteristic, while the spreading of plasticity through a grain boundary was found to somewhat retard the crack growth.

The authors Hansson, Melin and Persson [9] have developed a formulation which makes it possible to quantify zigzag crack paths emerging at crack growth through single shear and the initiation of such a short crack. It was found that the initial crack angle determined the shape of the crack

and that the growth rate changed dramatically between the different cycles. Growth rate decreases just before the crack is about to change its growth direction and grows the fastest in the cycle just after it has changed its growth direction.

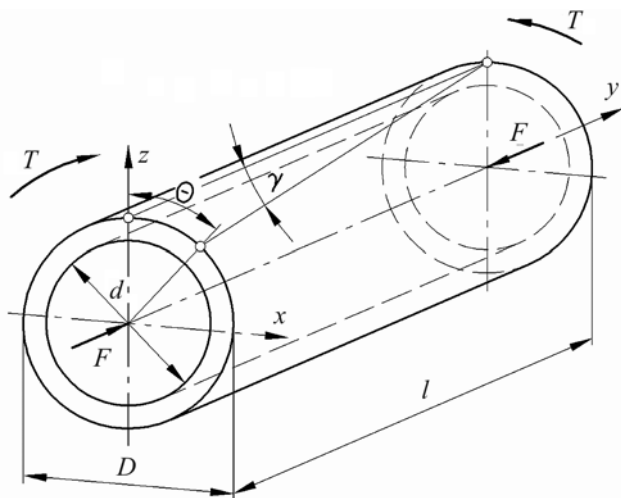


Figure 1 Compression force and torque on the tubular spring body
Slika 1. Opterećenje tlačnom silom i torzijskim momentom na tijelu cjevaste opruge

2 Testing material and spring samples

Ispitivani materijal i uzorci opruga

Testing samples of tubular torsion spring have been manufactured in accordance with design in Fig. 2 and Fig. 3. The applied spring steel has chemical composition shown in Tab. 1. Spring material was rolled, forged and soft annealed. The final shape was achieved by the following mechanical processes: deep drilling, honing, programmed turning, milling and polishing of the spring body to roughness of $Ra=0,2 \mu\text{m}$. Specimens were heat-treated by means of vacuum technology. The hardening temperature was of 870 °C, quenching with liquid nitrogen. Tempering lasted for 6 hours at the temperature of 220 °C. After hardening the tubular torsion spring specimens had mechanical properties shown in Tab. 2. The mechanical properties were determined by means of tension test. Specimens prepared for mechanical properties were made of the same material as the springs and they were treated together with the tubular torsion spring specimens. The mechanical properties of the material were compared with the testing results of the same steel [10].

Table 1 Chemical composition of the steel
Tablica 1. Kemijski sustav čelika

| Element | C | Si | Mn | Cr | Ni | Mo | V | Cu | P | S |
|---------|------|------|------|------|------|------|------|------|-------|-------|
| % | 0,44 | 0,28 | 0,56 | 0,87 | 1,41 | 0,26 | 0,11 | 0,12 | 0,009 | 0,002 |

Table 2 Mechanical properties of the steel
Tablica 2. Mehanička svojstva čelika

| Elastic Moduli | | Fracture Strain | Yield Stress | | Ultimate Strength | | Hardness |
|----------------|--------------|-----------------------|-------------------------|-----------------------|----------------------------|-----------------------------|----------|
| Tensile E/ Gpa | Shear G/ GPa | $\pm \epsilon_f / \%$ | $R_{p0,2} / \text{MPa}$ | τ_e / MPa | Tensile R_m / MPa | Shear τ_m / MPa | |
| 193 | 75,2 | 14 | 1570 | 801 | 2010 | 1192 | 52 - 55 |

Design of the tubular torsion spring was made in accordance with technology procedures for manufacturing

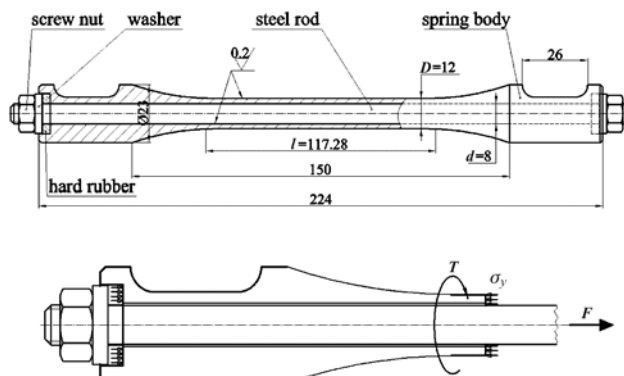


Figure 2 Torsion test specimen. Dimension in mm
Slika 2. Torzijski testni uzorak. Dimenzije u mm



Figure 3 Picture of torsion tubular spring specimen
Slika 3. Fotografija torzijske cjevaste opruge

industrial torsion bar springs. The tubular torsion spring is loaded in the axial direction on compression, and the bar inside the spring on tension, see Fig. 2. In such a way loading is concluded inside the construction. There is a potential danger of buckling due to spring's body compression load. However, the inside spring's wall can lean on a tension loaded bar and due to this the buckling is impossible. The danger of buckling is present also with full test pieces where compression axial force is re-established by means of testing machine outwards. In such a case only testing pieces shorter than the critical buckling length can be tested.

Testing torsion load was an alternating one or $R_\tau = \tau_{\min} / \tau_{\max} = -1$. The torsion stress amplitude was for all test samples the same $\tau_a = 640 \text{ MPa}$; expressed by factor $k_y = \tau_a / \tau_e = 0,8$, $\tau_a = k_y \cdot \tau_e$, where τ_e is a torsion elastic limit. The amplitude loading angle was in all test cases $\Theta = \pm 9,5^\circ$, while:

$$\Theta = 2\tau_a \cdot \frac{l}{GD} \cdot \frac{180}{\pi} \tag{1}$$

Where is $l=17,28 \text{ mm}$ a torsion length expressed in accordance with the standard DIN 2091, [11].

The amplitude loading torque was:

$$T = \frac{\pi \cdot (D^4 - d^4)}{16 \cdot D} \cdot \tau_a \tag{2}$$

Where is D an outside diameter and d an inside diameter of the hollow spring. The amplitude torque was 174,25 N·m.

During testing the tubular torsion springs were exposed to various constant axial stress as follows: $k_x=0,0$, $k_x=0,1$, $k_x=0,2$, $k_x=0,225$, $k_x=0,25$ and $k_x=0,3$, where relation k_x means a part of yield limit $\sigma_y = k_x \cdot R_{p0,2}$ and σ_y means axial stress at pre-stressing.

3 Testing device

Uređaj za ispitivanje

A device for fatigue testing of tubular torsion spring

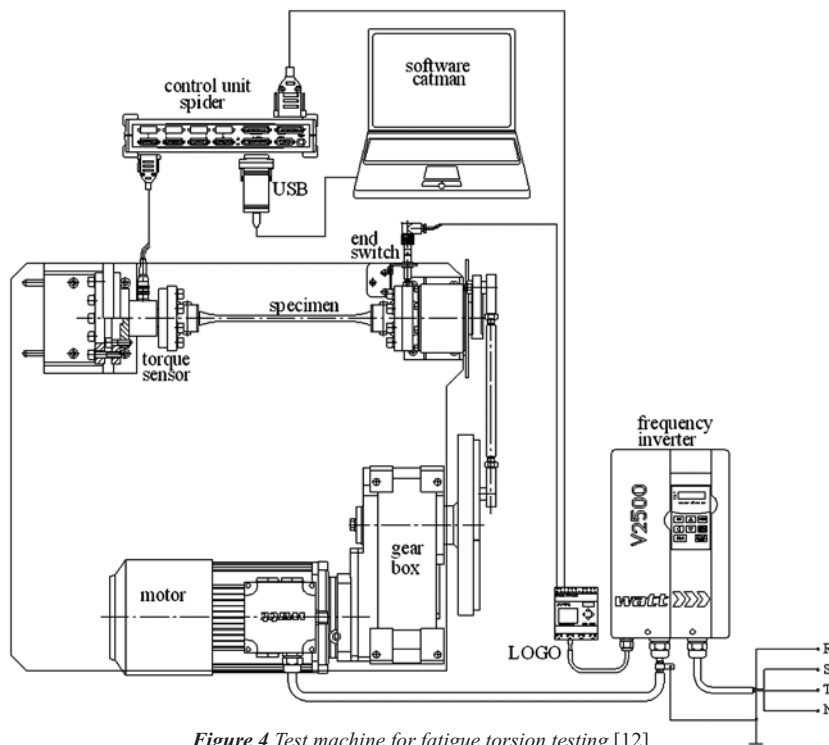


Figure 4 Test machine for fatigue torsion testing [12]
Slika 4. Uređaj za torzijsko testiranje na zamor [12]

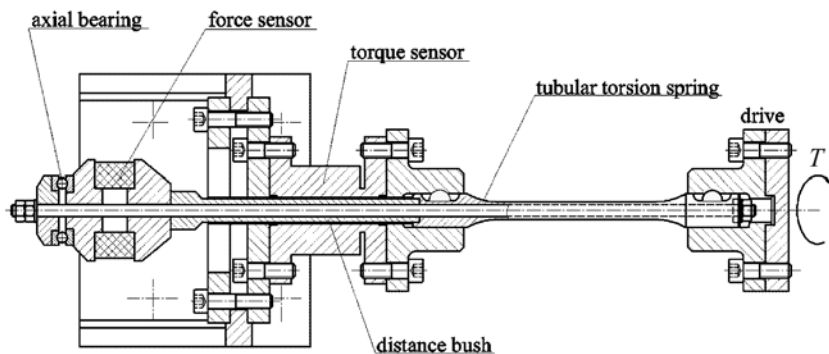


Figure 5 Clamping of a thin-walled tubular specimen during testing [12]
Slika 5. Princip stezanja tankostijene cjevaste opruge tijekom testiranja [12]

specimens has been designed and manufactured, Fig. 4. The device consists of a clamping unit, a driving unit and a measuring chain. Here the specimens of length up to 350 mm can be clamped. It is driven by an electric motor through an eccentric; speed is adjustable by means of frequency control. Testing frequency is 5 Hz at the most. The testing torque, twist angle, axial force and number of cycles are measured. Data processing commercial electronics Spider and software Catman are products of the company HBM. Fig. 4 shows a device for testing of specimens, and Fig. 5 the way of their clamping to ensure the control of the axial force during testing with the alternating torque.

4

Stress state in tubular spring specimen

Stanje naprežanja u uzorcima cjevastih opruga

In the tubular spring body biaxial stress state is formed during alternating torsion loading of the spring at simultaneous static axial force. The spring's wall is thin, therefore there is plane stress state applied. If the tube axle coincides with *y*-axle of the coordinate system, Fig. 1, the following stress tensor can be written:

$$\sigma_{ij} = \begin{Bmatrix} 0 & 0 & 0 \\ 0 & -\sigma_y & \tau_{yz} \\ 0 & \tau_{zy} & 0 \end{Bmatrix} \tag{3}$$

where σ_y means normal pre-stress in the spring's axial direction and $\tau_{yz} = \tau_{zy} = \tau_a$ is torsion stress. During loading cycle the torsion stress components keep changing in order of size, while the normal axial stress component stays unchanged. For the crack's initiation and growth principal stresses are decisive which can be written as follows in our case:

$$\sigma_{ij} = \begin{Bmatrix} \sigma_1 & 0 & 0 \\ 0 & 0 & 0 \\ 0 & 0 & \sigma_3 \end{Bmatrix}. \tag{4}$$

For the plane stress state the principal stress components can be written in the following way:

$$\sigma_{1,3} = \frac{1}{2} \cdot \left(\sigma_y \pm \sqrt{\sigma_y^2 + 4\tau_{yz}^2} \right). \tag{5}$$

The principal stresses lie in the tangential plane of the tube surface in an observation point, and their directions are as follows:

$$\tan 2\alpha_{1,3} = \frac{-2\tau_{yz}}{\sigma_y} \tag{6}$$

In Fig. 6 the principal stress vectors are shown in order of direction and size for positive and negative part of alternating torsion loading cycle. Due to continuous changing of torsion stress during loading cycle both principal stresses keep changing as well in order of size and direction. It is important that the principal stress directions change is affected by the torsion stress size, though normal axial pre-stress keeps unchanged during the loading cycle.

In Fig. 7 the change of principal stresses is shown during a positive part of loading cycle dependent on torsion stress and in Fig. 8a the change of the angles α and φ dependent on torsion stress during a halfway loading cycle. The principal stress direction is changeable only in the presence of axial pre-stressing, while it remains constant through whole loading cycle, if the springs without axial pre-stressing are in question, Fig. 8. Diagrams in Fig. 7 and Fig. 8 show an action on the outside circumference of the tubular torsion spring. The tangential stress component has its maximum there, and also stress concentrations occur due to the spring's surface roughness which can lead to a crack initiation.

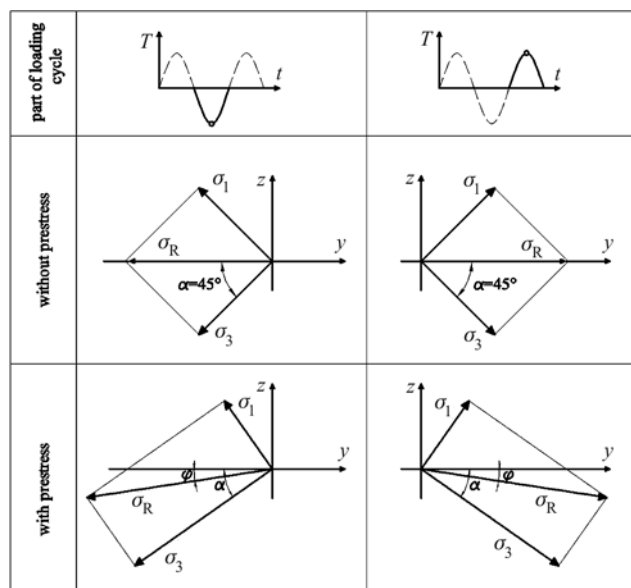


Figure 6 Principal stresses. Axle y is a longitudinal spring axle and σ_R is a resultant.

Slika 6. Glavna naprezanja. Os y je glavna simetrala torzijske opruge, σ_R je rezultanta.

The compression pre-stressing of the spring in the axial direction has a great effect on the spring's fatigue life enlargement. The testing results, Tab. 3, show an eight times enlarged fatigue life, and with the pulsating load the effect is essentially larger.

Compression stress in the axial direction closes initial cracks on the spring's surface and prevents their growth. The axial pre-stressing enlarges critical shear stress on slip planes in the material grain, which retards the nucleation of dislocation dipoles in the initial crack tips which are decisive for the growth of a micro crack through the grain. During the unloading process of the fatigue loading cycle

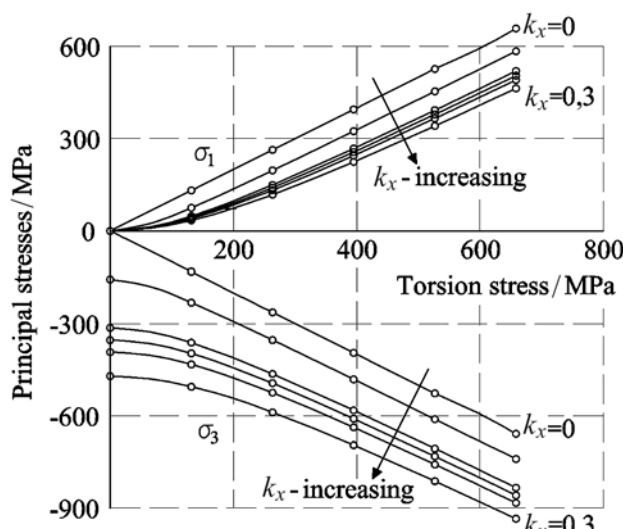


Figure 7 Principal stresses during positive part of loading cycle, dependent on torsion loading and ratio k_x

Slika 7. Glavna naprezanja tijekom pozitivnog dijela ciklusa opterećenja, ovisno o opterećenju i vrijednosti omjera k_x

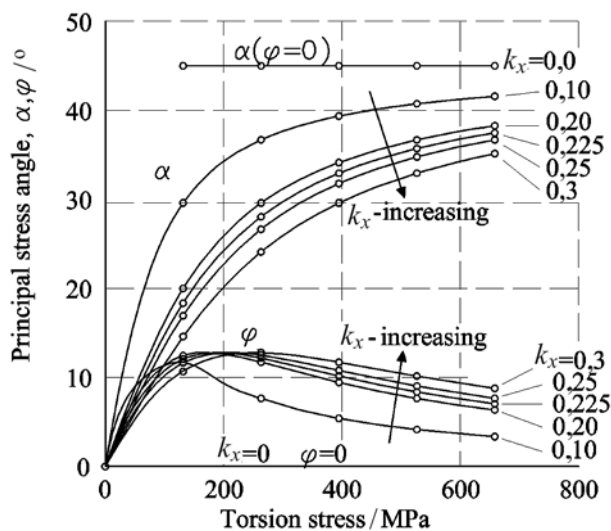


Figure 8 Principal stress angle α and φ , dependent on torsion stress and ratio k_x during positive part of loading cycle

Slika 8. Kutevi djelovanja glavnih naprezanja α i φ , ovisno o torzijskom naprezanju i vrijednosti k_x tijekom pozitivnog dijela ciklusa opterećenja

the compress stress obstructs returning of the discrete dislocations back towards the micro crack surface in the grain initial tip, which enlarges dislocation pile-up on the slip planes and consequently the static plastic zone around the crack tip is enlarged as well. The initiation process and the micro crack growth are slowed-down.

The second positive consequence and contribution to the spring's fatigue life is the stress state, unlike a spring without the axial pre-stressing. It is expected that the size of the principal stresses gets larger during the loading cycle when the torsion stress component is enlarged, but during the loading cycle their directions change as well at any moment. The principal stress action direction is constant with the springs without the axial pre-stressing, namely of 45° regarding the spring's direction, while with the axial pre-stressed springs the action angle changes continually during the loading cycle from 0 to approximately 42°. Due to the axial pre-stressing enlargement the principal stresses action angle gets smaller, at pre-stressing $\sigma_y = 0,3 \cdot R_{p0,2}$ the reached amplitude angle of the principle stresses is only of 35°, Fig. 8.

With the springs without axial pre-stressing the principal stresses act during the loading cycle all the time in the same direction. Inside the grain the slip planes get activated gradually according to the principle stress directions. During the loading cycle the dislocation process of micro cracks growth inside the grain continues. During repeated loading cycles micro cracks grow in accordance with the dislocation mechanism, new slip planes get activated and discrete dislocations move along them and after that partially form a static plastic zone and partially return on the micro cracks surface where they get annihilated, they re-sharpen the micro crack tips and prolong them for an appropriate number of Burger vectors, [8, 9]. The new slip planes get activated together with nucleation of new dislocation dipoles when the load during the loading cycle grows. The outside loading thus affects moving of the newly formed dislocations on the new slip planes, as well as moving of the dislocations on the slip planes activated during past moments of the same loading cycle and during past loading cycles.

With the springs with axial pre-stressing the same processes for the micro cracks growth go on in the grains. Due to changing the loading direction the newly activated slip planes correspond to the loading direction and size at the given torque, meaning that the loading with changed direction has less influence on the dislocations moving along the slip planes which were activated during past load increments of the same loading cycle and were in accordance with a different loading direction. The present loading can in such a way affect moving of the previously formed dislocations on their slip planes only with a defined component. Resulting from this more loading cycles are needed for the same irreversible processes inside the grain in the case of axial pre-stressing than in the case without it. The loading works less oriented or concentrated and therefore nucleates a large number of dislocation dipoles on several differently directed slip planes. The micro cracks progress in material in various directions, but less intensively than in the case when the spring was not axial pre-stressed. Lots of discrete dislocations cannot return to the cracks surface, which results in a larger plastic front extended around the micro cracks and later along the macro crack. Thus the micro structurally short fatigue cracks are arrested.

5

Testing results

Rezultati ispitivanja

Table 3 Spring's fatigue life dependent on ratio k_x at $k_y=0,8$

Tablica 3. Životni vijek trajanja opruga ovisno o vrijednosti k_x kod $k_y=0,8$

| x | 0,0 | 0,1 | 0,2 | 0,225 | 0,25 | 0,3 |
|-----------------------------------|--------|---------|---------|---------|---------|---------|
| Number of cycles till destruction | 46 059 | 165 554 | 307 442 | 295 050 | 353 758 | 257 324 |
| | 48 516 | | 319 108 | 328 942 | 407 801 | 312 813 |
| | 56 566 | | 356 023 | 352 034 | | 339 642 |

6

Fatigue crack on spring specimen

Zamorna pukotina na uzorcima opruge

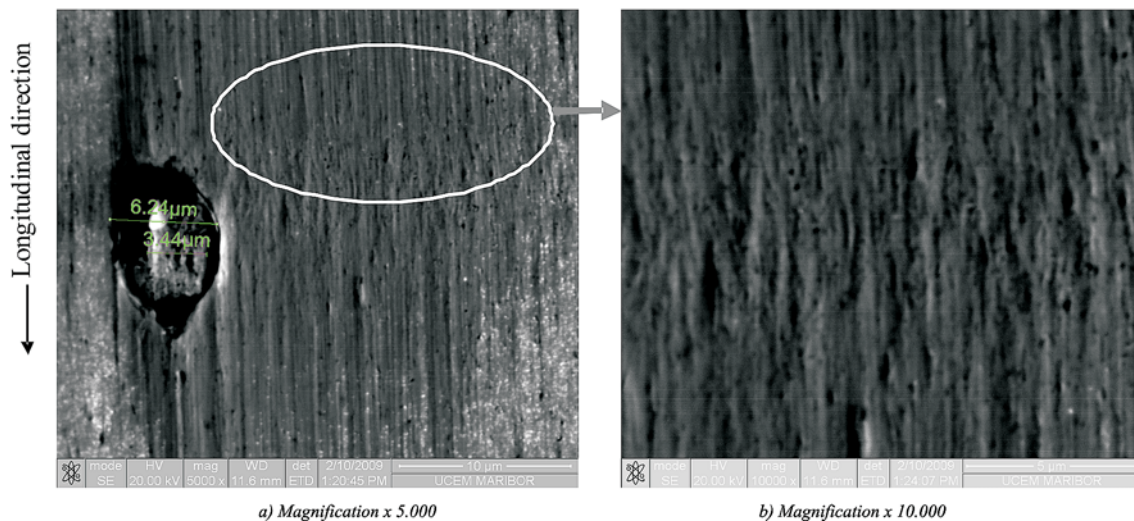
It has been mentioned that a quality industrial material was used during these investigations. Such a material with a fine martensitic-bainitic microstructure contains inclusions of MnS, Al₂O₃ and other oxides (e.g. TiO) as a consequence of the manufacturing process. The size of the inclusions was

usually less than 5 microns. However, the inclusions in the material present a potential site for the origin of a fatigue micro-crack if the deformation around them is locally significant. This is the case if the fatigue load is close to the yield stress, or a surface defect can locally increase the stress concentration. Such a concentration zone is possible to be found because there is irregular roughness on the surface of specimen. This irregular rough area has been generated during the fatigue test and becomes a high strain concentration zone.

The highest deformation occurs on the surface of a specimen as a consequence of the torsion loading. Figures 9.a and 9.b show such an irregular zone of around 3,1 microns size. The irregular rough zone also creates more small holes on the surface of the specimen. This is a consequence of the small inclusions (less than 0,5 μm). Fig. 10 schematically shows the fatigue micro-crack initiation process.

Thus, the process leads to the separation of material around inclusions and the formation of voids which generate micro cracks. Additional fatigue micro crack initiation results from the coalescence of voids. This is shown in Fig. 11. The direction of the fatigue micro-crack initiation under tension-compression loading is transverse to the main centre line of the specimen. After a shear crack reaches a length of several hundred microns, crack branching occurs along $\pm 45^\circ$ planes and the fatigue macro-crack propagation continues in the same manner for either high-cycle fatigue or low-cycle fatigue. Fig. 12.a shows the fatigue crack propagation direction from the initial shear crack (on the x axis) for different compression pre-stress levels ($k_x=0,1, 0,2$ and $0,3$). The initial shear crack is longer for a lower compression pre-stress ratio. Fig. 12.b shows macro crack branching. It is reasonable that the fatigue shear crack starts around larger inclusions, but also in case of small inclusions the fatigue shear crack is initiated in the same manner. However, the number of cycles for shear crack initiation is higher in the case of smaller inclusions.

Figures 13.a, 13.b and 13.c show the macro crack growth under a torsion loading for a constant static compression pre-stress ($k_x=0, 0,2$ and $0,3$) respectively. Fig. 13.a shows that the macro crack growth remains in the same plane, a transverse plane, as the initial shear crack in the case of pure torsion loading, that means in the maximal torsion stress direction. Fig. 13.b shows that after the shear crack reaches the length of several hundred microns, it branches along $\pm 45^\circ$ planes, but the material still remains on the surface of the specimen. This indicates that the crack growth is initially controlled by the largest shear stress, but later by the principal stresses. The initial crack length in the transverse direction depends on the axial pre-stress level. At an axial pre-stress of $\sigma_y=0,1 \cdot R_{p0,2}$ the initial crack length is about 0,7 mm, and at an axial pre-stress of $\sigma_y=0,3 \cdot R_{p0,2}$ it is about 0,2 mm, meaning that the higher the axial pre-stress imposed on the hollow torsion spring, the shorter the initial crack's distance and vice versa. Fig. 13.c shows high deformed material goes out of the specimen's surface under a higher static compression pre-stress $k_x=0,3$. This contributes to the reduction of number of cycles to final failure. Thus, an optimum compression static stress level exists for biaxial loading, because the higher compression pre-stress results in a lower fatigue life. Therefore, the optimum compression pre-stress depends on the stress-strain conditions of the component, and the applied stress magnitude and direction.



a) Magnification x 5.000
 b) Magnification x 10.000
Figure 9 Fatigue crack voids initiation process on the surface of a specimen [12, 13]
Slika 9. Proces inicijacije zamorne pukotine na površini uzorka [12, 13]

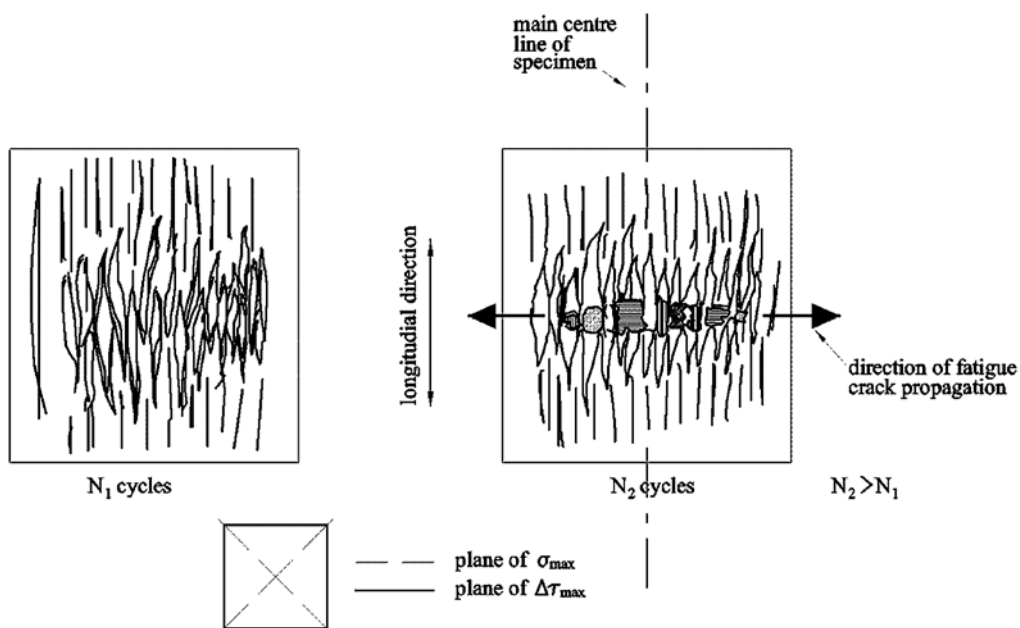


Figure 10 Schematic explanation of fatigue shear crack initiation in transversal direction regarding the main centre line of specimen [12, 13]
Slika 10. Shematski prikaz inicijacije smične zamorne pukotine poprečno u odnosu na glavnu simetralu uzorka [12, 13]

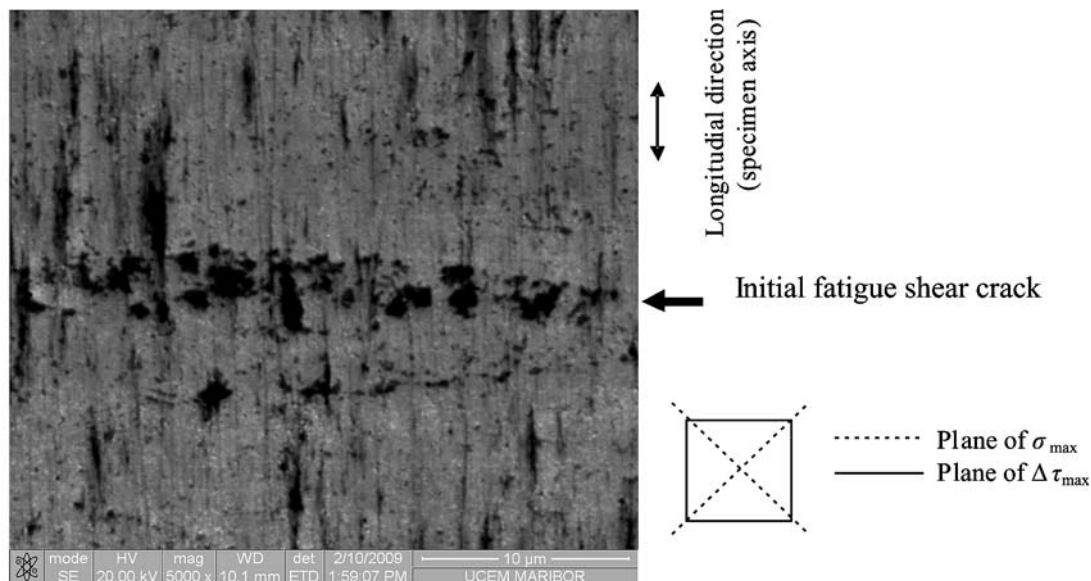


Figure 11 Behaviour of shear crack under torsion-compression loading showing coalescence of voids in transversal direction [12, 13]
Slika 11. Ponašanje smične pukotine pod utjecajem torzijsko tlačnog opterećivanja ukazuje na povećanje šupljina u poprečnom smjeru [12, 13]

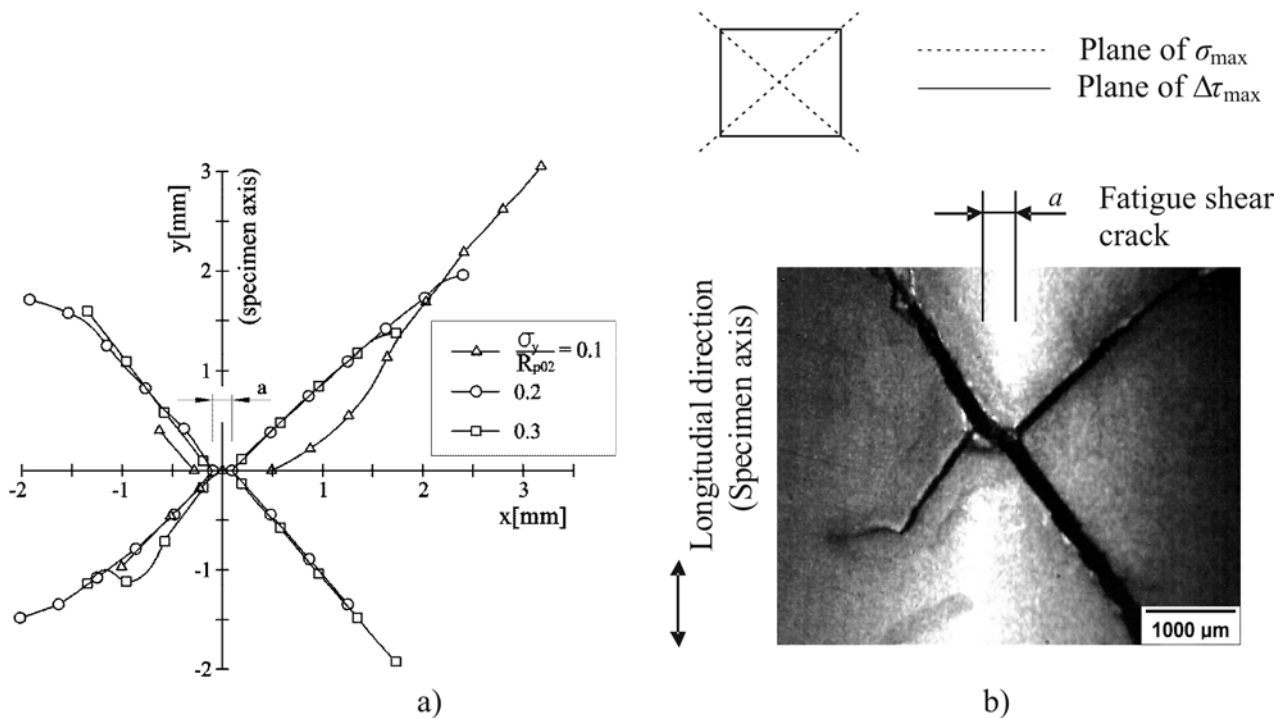


Figure 12 After a shear crack reaches a length of several hundred microns, the crack branching along $\pm 45^\circ$ planes occurs (examples for compress stress levels $k_x=0,1, 0,2$ and $0,3$) [12, 13]

Slika 12. Kada smična pukotina postigne duljinu od nekoliko stotina μm , grane pukotine počnu se širiti u smjeru od $\pm 45^\circ$ (primjeri za tlačna naprežanja za omjere $k_x=0,1, 0,2$ and $0,3$) [12, 13]

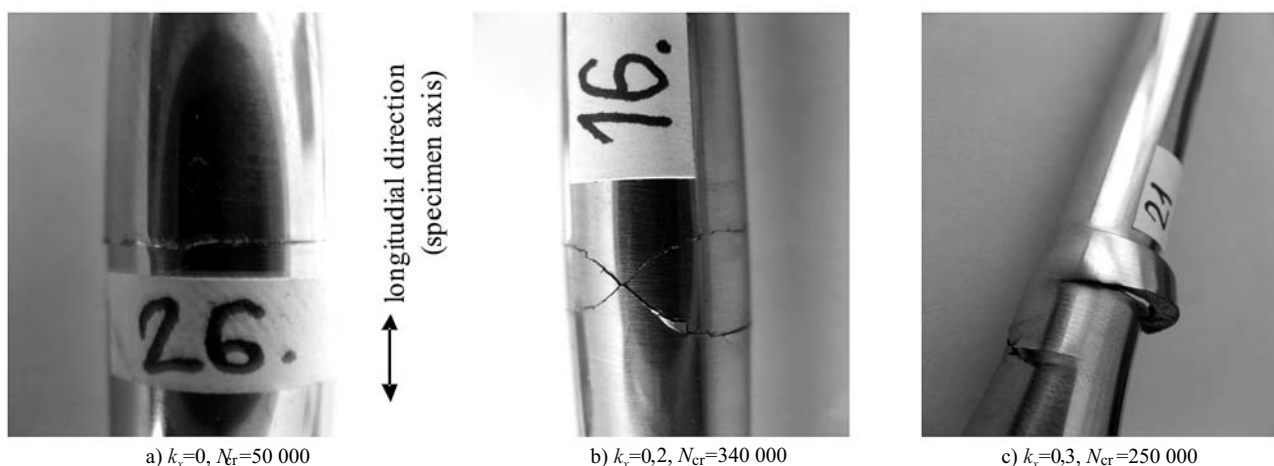


Figure 13 Macro crack growth under torsion loading with regard to constant static compress stress σ_x [12, 13]

Slika 13. Rast makropukotine pod utjecajem torzijskog opterećenja u odnosu na konstantni omjer tlačnog naprežanja σ_x [12, 13]

With a specimen loaded in torsion from zero to maximum stress and without axial pre-stressing, $k_x=0$, the macro crack grows in a spiral path at an angle between 28° to 44° ; this coincides to the principal stress direction, 45° . When the torsion loading is directed to the right, the crack's spiral goes right, and vice versa.

Fig. 14 shows the strain life limit curve for a surface roughness of $Ra=0,2\ \mu\text{m}$ and for a roughness of $Ra<0,1\ \mu\text{m}$, respectively. True principal strain is given on abscise x , while the ordinate y , gives the logarithmic value of the number of cycles for fatigue failure (visible crack extension on the surface or a 10 % drop in the moment, whichever occurs first). Each point on the curves is experimentally obtained. Fig. 14 shows that the static compression pre-stress increases fatigue strain life for true strain within the range of $85,4 - 87,4\%$ of the true yield strain. An increase in the strain life of more than 7 times is possible with a compression pre-stress of $k_x=0,25$, but an increase of more than 10 times is possible by additionally limiting the surface roughness to $Ra<0,1\ \text{mm}$.

In practice, it is already well known that surface roughness plays an important role but it is not often reported how the fine grinding can improve fatigue life for low-cycle fatigue behaviour. However, this investigation confirms that the shear crack initiates on the smooth surface of a similar roughness quality if the specimens are subjected to torsion loading.

6 Conclusions Zaključci

The paper deals with the behaviour of the alternating torsion loaded tube springs at simultaneous presence of constant compression stress in the spring's axial direction. Design, material, the way of manufacture and the way of the springs' testing are represented. Furthermore stress state during one loading cycle of an axial pre-stressed spring, a pre-stressing effect on the spring's fatigue life and

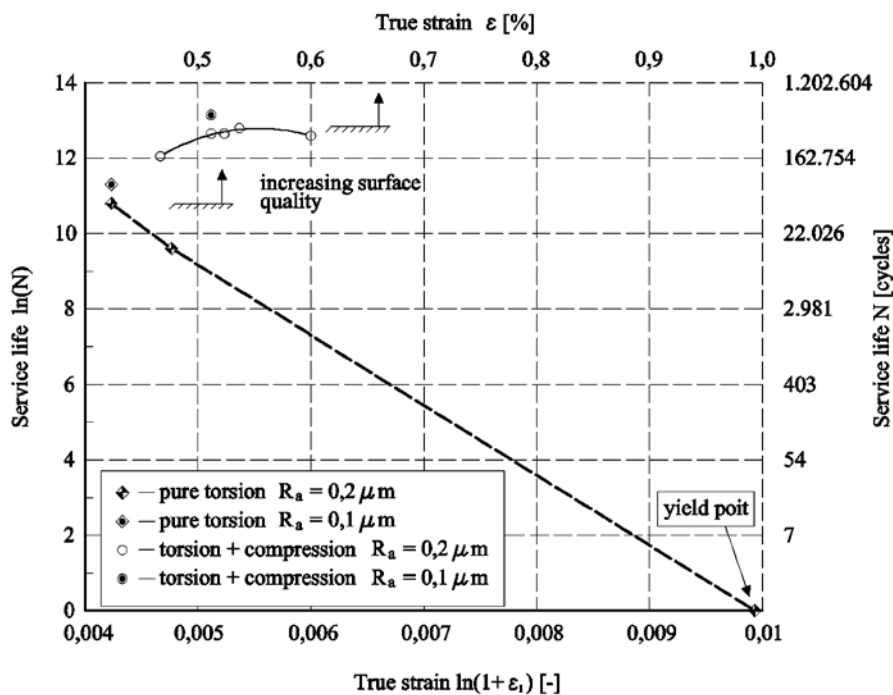


Figure 14 Strain life limit curves for two different surface roughness values with a maximum life with a range 86,4 % of true strain [12, 13]

Slika 14. Granične krivulje deformacijskog životnog vijeka za dvije kvalitete površinske obrade za maksimalan vijek u rasponu od 86,4 % stvarne deformacije [12, 13]

consequently formation, shape and geometry of the macro crack are treated. The following is stated:

- 1 A new design of torsion fatigue loaded tube springs has been suggested. The spring's fatigue life enlargement has been achieved by pre-stressing in the tube torsion spring's axial direction.
- 2 The tube torsion springs are safer for application because of gradually growing fatigue crack due to plane stress state, while with the full torsion bar springs due to plane deformation state the spring is destructed unexpectedly.
- 3 In the axial pre-stressed tube torsion spring a biaxial stress state occurs in which the principal stresses σ_1 and σ_3 change in order of size and direction during torsion loading cycle.
- 4 The spring's fatigue life is enlarged due to the following factors:
 - a) Compression stress in the axial direction prevents the surface initial cracks from growing.
 - b) Compression stress in the axial pre-stressed tube torsion spring enlarges critical shear stress for dislocation dipoles nucleation and discrete dislocations moving on the slip planes inside the grain and in such a way the micro cracks' growing inside grains is slowed-down.
 - c) Inside the grain new slip planes are activated all the time during the loading cycle and they are each time in accordance with a new direction of the principal stress. Due to changing direction of the principal stresses during the loading cycle less dislocation dipoles are nucleated on individual slip planes inside the grain. Principal stress direction changing affects slow-down moving of discrete dislocations on slip planes in the grain due to resolving shear stress causing the discrete dislocation moving on slip planes at any subsequent moment due to changed direction only with a definite component. The discrete dislocations return slowly to

the crack tips during unloading and in such a way form a plastic zone around the micro crack tips. For this reason several more loading cycles are needed for the micro cracks growing to prolong the spring's service life.

- 5 With the tube torsion springs without axial pre-stressing and without the initial notch, being alternating torsion loaded, a micro crack continues in the transversal direction that is direction of the maximum shear stresses. In the case of the axial pre-stressing at first a short initial crack in transversal direction is formed, and then it continues in the shape of the left and right spiral along the spring. The initial macro crack's length gets smaller with increasing the axial pre-stressing and vice versa. At the beginning the crack's spiral with a longitudinal axle y forms an angle ranging about 45°.

7 References Literatura

- [1] Milinković, B. Pomeranje granice elastičnosti torzionih štapova primenom prethodnog naprezanja. // Naučno-tehnički pregled vol. XXXIV. 6, (1984), str. 16-25.
- [2] Tschegg, E. K. A contribution to mode III fatigue crack propagation. // Mater. Sci. Engng. 54, (1982), str. 127-136.
- [3] Fonte, M. A.; Freitas, M. M. Semi-elliptical fatigue crack growth under rotating or reversed bending combined with steady torsion. // Fatigue Fract. Engng. Mater. Struct. 20, (1997), str. 895-906.
- [4] Zang, W.; Akid, R. Mechanisms and fatigue performance of two steels in cyclic torsion with axial static torsion/compression. // Fatigue Fract. Engng. Mater. Struct. 20, (1997), str. 547-557.
- [5] Makabe, C.; Socie, D. F. Crack growth mechanisms in pre-cracked torsion fatigue specimens. // Fatigue Fract. Engng. Mater. Struct. 24, (2001), str. 607-615.
- [6] Yang, F. P.; Kuang, Z. B. Fatigue crack growth for a surface crack in a round bar under multi-axial loading condition. //

- Fatigue Fract. Engng. Mater. Struct. 28, (2005), str. 963-970.
- [7] Tanaka, K. and Iwata, Y. and Akiniwa, Y. Fatigue Crack Propagation in Lead- Free Solder under Mode I and II Loadings. // 17th European Conference on Fracture. Brno '08, Czech Republic, September 2-5, 2008, str. 1008-1015.
- [8] Bjerken, C.; Melin, S. Modelling and simulation of short fatigue cracks, Doctoral thesis. // Division of Materials Engineering, Lund University, Sweden, 2003.
- [9] Hansson, P.; Melin, S.; Persson, C. Dislocation modelling of short fatigue crack growth through shingle shear, Licentiate Dissertation. // Department of Mechanical Engineering, Lund University, Sweden, 2004.
- [10] Dobi, Đ. Ciklične karakteristike jekla TORKA. Ustvarjalna naloga Železarna Ravne, Ravne na Koroškem, 1987.
- [11] DIN 2091. Drehstabfedern mit rundem Querschnitt, Berechnung und Konstruktion, DK 62-272.5, 1981.
- [12] Močilnik, V. Vpliv prednapetja na dinamično nosilnost vzvojnje vzmeti = The Influence of Pre-Stress on Dynamic Capacity of the Torsion Spring, Doctoral thesis. // University of Maribor, Faculty of Mechanical Engineering, Oct. 2009.
- [13] Močilnik, V.; Gubeljak, N.; Predan, J.; Flašker, J. The Influence of Constant Axial Compression Pre-Stress on the Fatigue Failure of Torsion Loaded Tube Springs. // Engineering Fracture Mechanics, Accepted 19 July 2010. Available online 27 July 2010. (It will be published in the Volume 77, Issue 16, November 2010, Pages 3132-3142).

Authors' Addresses

Adrese autora

Dr. Vinko Močilnik

Engineering Biro
Vinko Močilnik s.p.
Črneče 186
2370 Dravograd, Slovenia
e-mail: vinko.mocilnik@siol.net

Prof. Dr. Nenad Gubeljak

Fakulteta za strojništvo
Univerze v Mariboru
Smetanova ulica 17
2000 Maribor, Slovenia
e-mail: nenad.gubeljak@uni-mb.si

Dr. Jožef Predan

Fakulteta za strojništvo
Univerze v Mariboru
Smetanova ulica 17
2000 Maribor, Slovenia
e-mail: jozef.predan@uni-mb.si

Prof. Dr. Jože Flašker

Fakulteta za strojništvo
Univerze v Mariboru
Smetanova ulica 17
2000 Maribor, Slovenia
e-mail: joze.flasker@uni-mb.si